

Effect of Heat Treatment and Ceria Coating on the Degradation Behavior of 7075 Al/B₄C Composite in Red Sea Environment

Rajasekaran Saminathan*, Haitham Hadidi, Mohammed Tharwan,
Yahya Ali Fageehi and Ali Alnujaie

Department of Mechanical Engineering, Jazan University, Kingdom of Saudi Arabia

*E-mail: rsaminathan@jazanu.edu.sa

Received: 23 May 2022 / Accepted: 30 June 2022 / Published: 27 December 2022

7075Al/B₄C composites have been designed and developed since they have greater potential to be used in various industries especially in aerospace firms. In general the mechanical properties of the precipitation strengthening enabled Aluminum alloys are executed by means of artificial aging leading to precipitation strengthening. This work aims at a detailed analysis of the influence of artificial aging heat treatment on the degradation pattern especially corrosion behavior of 7075Al/B₄C composites in Red Sea environment. Stir casting methodology is used to manufacture the composite using 7075 Aluminum alloy and 15 wt% B₄C particulates. Brinell hardness measurements were carried out further to find the hardness of artificially aged group of composites. The hardness profile is used to categorize the aged composites into under aged (UA), over aged (OA) and peak aged (PA). These groups are further tested in potentiodynamic polarization studies using AUTO LAB corrosion measuring instrument. The topographical responds of the composite specimens exposed to Red Sea Water, is studied using SEM, EDAX and XRD. It is registered that the peak aged composites show higher tendency to corrode in Red Sea Water in comparison with other categorize of artificially aged composites. The SEM micrographs reveal that the interface between the matrix and the reinforcements corrode along with the intermetallic precipitates. Ceria conversion coating observed to improvise the corrosion resistance characteristics of the composite to a greater level.

Keywords: Precipitation strengthening, corrosion, cerium coating, artificial aging, Red Sea Water.

1. INTRODUCTION

Design of Aluminum alloys were carried out with view of achieving desired mechanical properties especially high strength to weight ratio for various industries including marine, automobile and aerospace industries [1-5]. In the design of alloying process addition of alloying elements to aluminum leads to discontinuation of the intrinsic oxide layer of Aluminum, which increases the rate at which corrosion processes can occur. Due to the topographical disturbance of homogeneity, the passive

oxide layer has discontinuities and hence the chance of corrosion reactions with atmosphere increases. Also to achieve tailor made properties of the Aluminum alloys due to various needs of the industries, inclusion of ceramic natured particulates as reinforcements like SiC, Al₂O₃ and B₄C were employed to manufacture Aluminum based metal matrix composites (MMCs) [6,7]. The presence of reinforcements in the matrix as well as the intermetallic precipitates give rise to adversarial consequence on the surface chemical stability of the aforementioned composite material in aggressive environments [6,8]. In the view of enhancing the mechanical properties like strength and hardness, these composites are subjected to artificial aging since the alloy comes under heat treatable category. The heat treatment procedure starts with solution treatment at a temperature just below to the melting point of the alloy for a specific time period followed by quenching to achieve single phase solid solution and then artificial aging at relatively lower temperature ranges to enhance the intermetallic precipitate formations. Since the precipitation strengthening is the major phenomena behind the strengthening mechanism, the parameters of the heat treatment like time of soaking and temperature of soaking decide the extent to which the mechanical properties are improved by means of altering the size and shape of the secondary phase precipitates. This in turn influences the mechanical as well as the corrosion properties of the composites [9-11]. Red Sea happens to geologically be present in between the Asian region and African region. Hence the water current leads to varying water circulation pattern and complex saline nature when compared to that of other oceans. The corrosion behavior of metallic alloys and concerned metal matrix composite materials in red sea environment are not completely studied and published in literature [12]. The literature review clearly suggest that there is a scope for the analysis of the consequence of intermediate temperature aging on the corrosion behavior 7075Al/B₄C composites in Red Sea environment. This study aims to carry out the artificial aging treatment of the composite and then investigating the post heat treatment consequences on the degradation pattern of the aforementioned composite in Red Sea environment.

2. MATERIALS AND METHODS

2.1. Material

The metal matrix composite (MMC) of consideration of this work is 7075 Al/B₄C composite. Stir casting technique is utilized to prepare the composite material. The alloy 7075 elemental constitutions are shown in the following Table 1. Organ gas pumping inlet option is attached to the furnace to execute organ flow at the rate of three liters per minute. The inert argon gas pumped furnace is heated to 890 °C to generate inert atmosphere with in. The inert gas arrangement ensures the magnesium present in the alloy does not get burned due to high temperature exposure. Further the measured quantity of the alloy is introduced in a crucible to the furnace. Sufficient time is allowed for the alloy to get transferred to molten state. Further the B₄C particles (22 μm in size) of measured quantity are introduced gradually into the molten alloy while the stirrer is operating [13]. The wettability of the aforementioned particulates in the 7075 molten alloy is poor and care is needed to improve the same by using higher rpm of 800 for a prolonged time period of 60 minutes. This ensures achieving uniformity in reinforcement distribution and the improved wettability of the particles. There is a need to make sure

rapid cooling does not occur when the molten liquid with particulate reinforcement is transferred into the die. Hence pre heating of the die made of steel is carried out at 400 °C for a time duration of 30 minutes. Sufficient time is allocated for the cast structure to get cooled to the ambient temperature and then test coupons of size equivalent to 2cm x 2cm x 2cm are cut using CNC cutting machine. The cut coupons are subjected to precipitation hardening heat treatment.

Table 1. Elemental constituents details

Elements	Cr	Cu	Fe	Mg	Mn	Si	Ti	Zn	B ₄ C	Aluminum
Wt %	0.29	2	0.6	2.3	0.29	0.33	0.15	5.1	15	Remaining

2.2. Age hardening of the composite

The artificial aging involves solutionising the specimen at a temperature just below to melting point in order to achieve single phase solid solution and followed by aging at intermediate temperatures. At 520 °C the aforementioned composite coupons are solution treated for a predetermined time of 60 minutes and then followed by quenching in water. A resistance heating furnace is used for hardening heat treatment experiments. The time gap between removal of specimens from furnace to introduction to water is only few seconds. Further the coupons are divided to 6 groups to carry out intermediate temperature aging from 80 to 160 °C in steps of 20 °C for different durations. Additionally the composites coupon are polished using various grades of SiC polishing sheets. This is executed up to 1000 grade paper. In continuation of the polishing, the paper polished coupons are subjected to wet polishing on velvet cloth using 3 µm grit with diamond paste. Then the wet polished coupons are degreased using ultrasonic bath treatments. According to the specifications of ASTM standards E10, the hardness variations of the aged group of composites are tested by Brinell Hardness Measurements. In the test, the indenter of 10 mm diameter is selected and 1500 kgf is opted. Application of load on the polished surface of the specimen was set for 30 seconds. In order to minimise errors in hardness measurements, ten reading are taken on every specimen and the corresponding average is considered as hardness of the specimen. A complete hardness profile of the heat treated coupons is plotted between time of aging and hardness values. The comprehensive plot consisting of three variables namely time of aging, temperature of aging and hardness values reveals the hardness variations as shown in Fig.1. Depending on the variations of hardness the coupons are categorized into three groups. They are namely PA corresponding to aging for 60 hours at 120 °C with measurement of hardness nearly 1400 MPa, UA corresponding to aging for six hours at 80 °C . OA specifies the coupons aged at 160 °C for 40 hours.

2.3. Ceramic conversion coating

Due to the fact that the PA composites show improved mechanical behavior, peak aging would be adapted for most of the engineering applications involving the aforementioned composite. The PA samples had their surfaces polished to a grit of 2000 using silicon carbide (SiC) abrasive sheets prior to treatment. Afterwards, the specimens were chemically treated to prepare them for the next step. Immersing the specimens in a NaOH solution with a pH of 12 for one minute at room temperature degreased them. For 40 minutes at 303 K, the pretreated samples were coated with a cerium-based conversion coating. NaAc + HAc was used to modify the solution's pH to 2.75, which was maintained throughout the coating process. After every process, the apparatus was cleaned with deionized water. Dissolving 7.5 grams of CeCl₃ in 1000 mL of deionized water having a 120 mL/L H₂O₂ concentration yielded a typical coating solution (Ce:H₂O₂ molar ratio of 1:50). Using a 30% H₂O₂ solution, the bath solution was prepared. The coating solution was applied to the pretreatment samples for 30 minutes, and they were then allowed to dry in the open air. The coated specimens were dried in ambient condition for two hours. Electrochemical testing is performed on the cerium oxide-coated PA composite specimens. A potentiostat controlled by software was used to conduct electrochemical measurements.

2.4 Electrochemical testing

Solution treated (ST), UA, OA, and PA composite coupons are paper polished using several grades of SiC polishing sheets up to 2000 grit followed by cloth polishing using to 3 μm sized diamond paste. After cloth polishing the coupons are degreased in ultrasonic bath before introduction to Red Sea water and 3.5 M sodium chloride solutions at room temperature, namely 28 °C, during electrochemical testing. The Red Sea Water to be used as electrolyte in conduction of corrosion tests, is gathered 10 kilometers away from the sea shore of Jizan Beach in Saudi Arabia, to ensure that the sea water is free of contaminants caused by the beach's human waste. Potentiodynamic polarization scans begin at -1100 mV vs SCE and end at around -100 mV. The corrosion rates were computed using Potentiodynamic polarization scans obtained over the range of 1100 to -100 mV using the AUTOLAB instrument. The scan rates for all Potentiodynamic polarization scans were 0.3 mV/s. The aforementioned electrochemical testing equipment was constructed up of a three-necked corrosion measurement cell, a stainless steel counter electrode, and a saturated calomel electrode (SCE) as a reference electrode. The SCE is used as the base reference to all measured potentials. Potentiodynamic polarization measurements were used to assess polarization resistances of the heat treated composite coupons.

Rate of corrosion is calculated using the formula furnished below. [14,15]

$$CR(mpy) = \frac{0.129 \times I_{CORR} \times Eq. Wt}{D} \quad \text{--- (1)}$$

Where, I_{corr} is the corrosion current density in microamperes per square centimeter.

Eq.wt depicts equivalent weight of the corroding sample. D represents Corrosion species' density in g/cm³.

The corrosion current density (I_{corr}) can be computed by dividing the corrosion current (i_{corr}) by the area of the specimen exposed to the electrolyte.

$$I_{CORR} = \frac{1}{2.3R} \left(\frac{\beta_a \beta_c}{\beta_a + \beta_c} \right) \dots (2)$$

Where,

R is representing Polarization resistance ($k\Omega/cm^2$)

β_a refers to Anodic slope (Volts/Decade) and β_c refers to Cathodic slope (Volts/Decade)

A JEOL JSM-6380LA SEM is utilized for topographical studies. The coupons were scanned using an X-RD instrument (JEOL JDX – 8P) with a copper (30kV, 20mA) target and a K filter.

3. RESULTS AND DISCUSSION

3.1. Intermediate temperature aging characteristics of the 7075 Al/B4C composites (T6 Treatment)

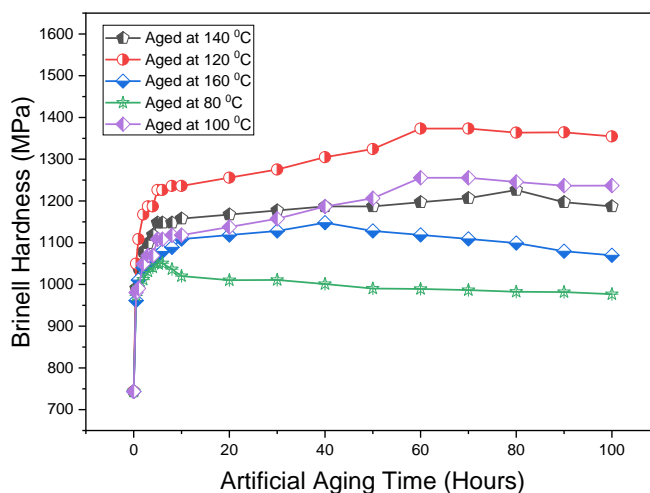


Figure 1. Brinell Hardness profile of Heat treated specimen

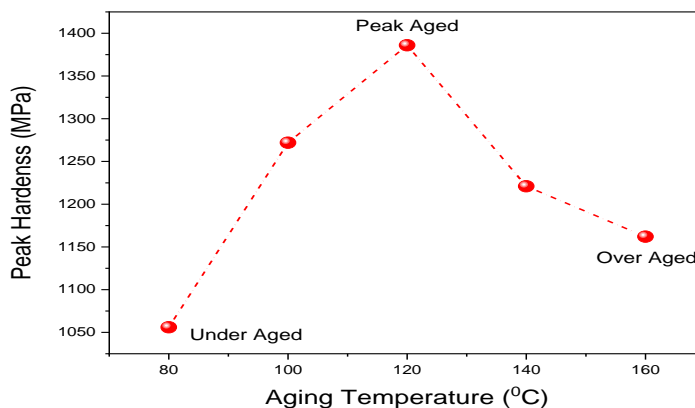


Figure 2. Dependence of Hardness of used samples on aging temperature (PA - 60 hours aging at 120 °C, UA- six hours aging at 80 °C . OA – 40 hours of aging at 160 °C).

Fig.1 depicts the variation in hardness in responds to artificial aging time at predetermined temperatures during the heat treatment. Figure 2 depicts the maximum hardness achieved during the intermediate temperature aging process over a range of temperatures. The one-hour solution treatment results in dissolution of secondary phase precipitates existing prior to heat treatment with in the matrix, changing it to a solid solution characterized by one phase containing all of the elemental additions in their own form. The saturated solid solution is retained at ambient temperature by means of executing the quenching in water medium. However, the super saturated solid solution is thermodynamically unstable, and the shift to a stable state initiates by forming precipitation nuclei. This process occurs automatically, and a longer duration is required for the complete formation of secondary phase precipitates [15,16]. When the alloy matrix gets the exposure to a preset temperature and duration during the artificial aging process, the precipitation phenomenon is getting accelerated. Asper metallurgical aspects, GP zone development occurs arbitrarily in the alloy matrix during intermediate temperature aging of Aluminum alloy containing Magnesium and Silicon, based composites from 80°C to 160°C. Further, the Guinier Preston zones gradually undergo transition into the unstable phase (η'), which is aided by thermodynamics. The process continues with the unstable phase (η') being transformed into the equilibrium phase (η) [15,17].

Coupons after the solution treatment are further subjected to intermediate temperature aging at temperatures ranging from 100 to 160 °C in steps of 20 °C increments during the artificial aging. The development of secondary phase nuclei by thermal energy supply triggers the beginning of precipitation process at this stage. As time of aging increases, the further generation of precipitating nuclei continues. The same phenomena continues to happen until the solid solution reaches the equilibrium state. The rate of phase transformation is determined by the length of time and temperature of the aging kinetics. As a result, the uniform existence and size of the secondary phase precipitates are entirely depend on kinetics parameters namely temperature and time period of aging, leading to alteration in the mechanical properties such as hardness. Furthermore, uniformly distributed precipitates have a strong tendency to suppress dislocation motion, which improves the matrix's mechanical characteristics. The fineness or coarseness of the precipitates in the alloy matrix is influenced by the duration and temperature of the heat treatment procedure followed. [18,19].

3.2 Corrosion Characteristics of the 7075 Al/B₄C composite

Originating GP zones with more or less spherical shape at the initial stages of the artificial aging treatment and grow in size as the heat treatment progresses. As the aging temperature rises, the critical ratio of Zn to Mg rises, resulting in the phase transitions. With varying Zinc Magnesium ratios, the heat treatment kinetics affects the generation of the GP zones. The hardness of the 7075 alloy matrix is shown to increase when the Zn to Mg ratio in the precipitate happens to increase [20]. Hence it can be stated that the resistance to indentation behavior of the aforementioned composite material is vastly influenced by the heat treatment's kinetics.

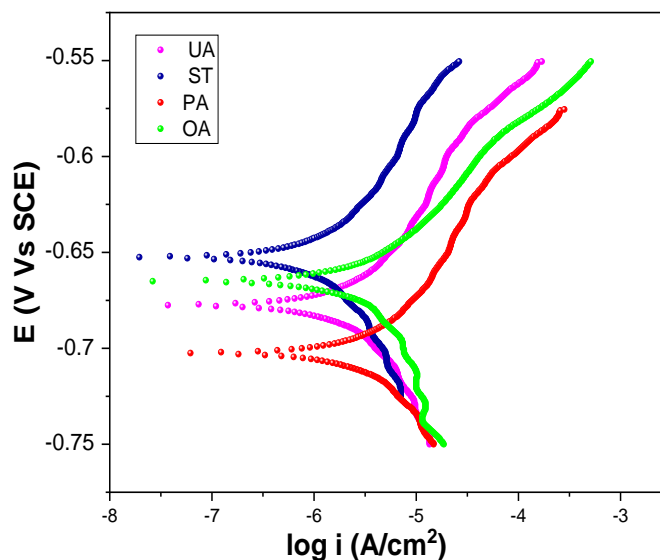


Figure 3. Potentiodynamic polarization plot of aged composite in sodium chloride solution

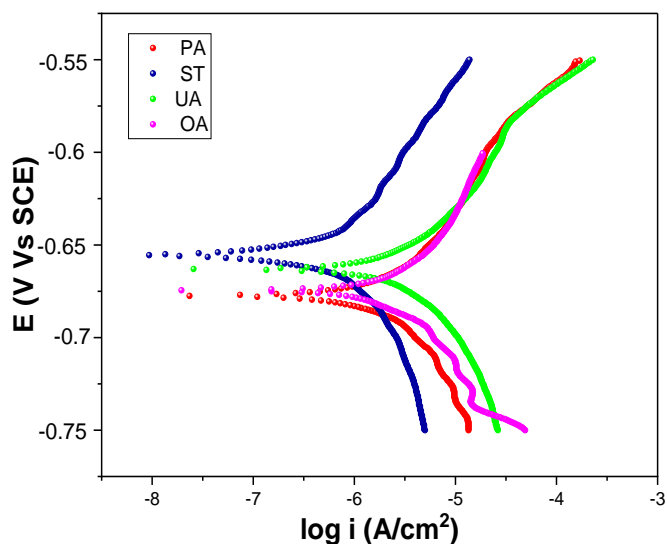


Figure 4. Potentiodynamic polarization plot of aged composite in Red Sea water where notations represent as follows UA – Under Aged, OA – Over Aged, PA – Peak Aged, ST- Solution Treated.

The Potentiodynamic polarization curves for artificially aging treated 7075 Al/B₄C composite containing 15 wt% B₄C in 3.5 M sodium chloride solution and Red Sea water are depicted in Fig 3 and 4. Table 2 show the registered corrosion parameters of the tests carried out. The potentiodynamic polarization curves furnished in figure 3 and 4 show a clear variation of shifting of the curves with respect to potential and current scale. In both cases, the curve of the peak aged composite happens to be at lower potential and higher current scale. Specific description of the former sentence can be obtained by analyzing the anodic and cathodic slopes meeting point giving rise to the corrosion current value of the curve. The coupons of the composites specified as PA group register with higher rate of corrosion

among all the groups of aged coupons. This can be correlated to the fact that differential kinetics of formation of intermetallic metallic precipitates at various aging time and temperature leading to enhanced strength as well as decrease in corrosion resistance. Also the peak aging leads to uniformity and finesse of the secondary phase formations in the alloy matrix. As a result the inhomogeneity of the matrix leads to instability of matrix itself upon exposed to aggressive chemicals [6,15, 21]. The inherent oxide layer development upon Aluminum surface protects it from chemical attacks. However, Aluminum is susceptible to dissimilar metal corrosion when alloyed with galvanically passive elements; Therefore, it can be stated that the alloy matrix in the case of Aluminum MMCs are vulnerable to corrosion when exposed to aggressive environments. The quantitative and qualitative nature of dissimilar metal corrosion of the alloy matrix depends on 1) the concentration and type of corrosive medium in contact 2) type and amount of reinforcing element to the matrix. Actually the reinforcement in the matrix creates large amount of grain boundaries which are higher energy regions, prone to electrochemical attack in aggressive media. In the stir casting stage, due to high temperature process there is possibility for reactions to occur between the matrix and the reinforcing phase leading to newer type of secondary phase precipitations to form.

Intermetallic precipitates formed during the manufacturing and in thermal treatment can influence the degradation behavior of the composite [21]. Actually the observed rates of degradation of the heat treated composite material coupons in Red Sea water is comparatively more in comparison with the same in 3.5 M NaCl solution. Because of the Red Sea's diverse saline character, this is possible [12]. Another interesting observation is that the shift of polarization curves of composite specimens tested in Red Sea water happens to be towards the lower potential and higher current scale. This describes that the composite has higher corrosion rate for the Red Sea Water whereas the same parameter happens to be lower in 3.5 M NaCl solution.

Table 2. The corrosion parameters of intermediate temperature aged 7075 Al/B₄C composite

Material	Corrosion potential (E _{corr})		Polarization resistance (R _p)		Corrosion current density (I _{corr})		Corrosion rate	
	mV Vs SCE		(kΩ/cm ²)		(μA/cm ²)		(Mils/year)	
	3.5 M NaCl	Red Sea water	3.5 M NaCl	Red Sea water	3.5 M NaCl	Red Sea water	3.5 M NaCl	Red Sea water
ST	-666	-665	5.23	4.23	7.49	9.13	3.57	4.12
OA	-671	-669	4.45	3.78	8.21	10.23	3.91	4.37
UA	-678	-675	3.98	2.34	8.97	9.89	4.34	4.67
PA	-703	-683	2.79	2.01	9.51	11.67	5.45	6.78
CeO ₂ Covered	-721	-702	6.72	5.34	5.23	6.76	1.94	2.46

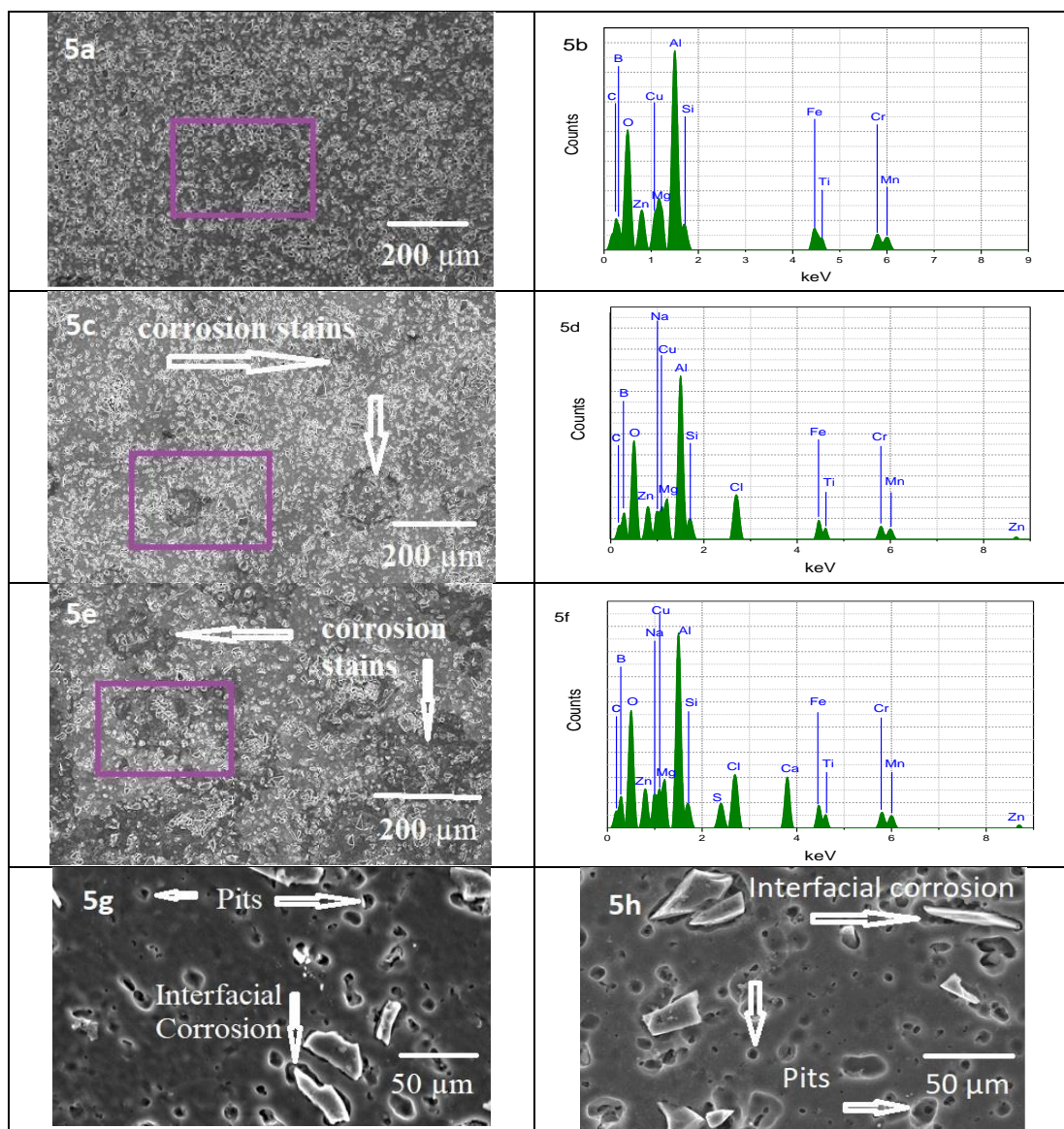


Figure 5. Topographical analysis of the 7075 Al/B₄C composite using SEM and EDAX.

3.2.1 Topographical analysis of the 7075 Al/B₄C composite

The surface chemical responds of the heat treated 7075 Al/B₄C composite specimens upon exposures to 3.5 M NaCl solution and Red Sea water are furnished in Fig.5. The 5a shows the SEM micrograph of the composite in polished and etched condition. The corresponding EDAX profile (5b) reveals the presence of Boron, Carbon, Aluminum, Oxygen, Magnesium, Manganese, Zinc, Chromium, Titanium etc.,. The composite exposed to atmosphere develops a thin oxide layer on its surface showing a peak of oxygen in EDAX profile. Figure 5c depicts the composite surface after the Potentiodynamic polarisation test in 3.5 M NaCl solution exhibiting the stained regions all over the surface. This shows that the surface of the composite gets corroded uniformly and galvanically since the potentially differing elements in galvanic series are added to the Aluminum matrix. The corresponding EDAX profile (5d) furnishes the presence of Na and Cl peaks apart from the peaks of other elements, due to the corroded products existence on the topography of the composite. Figure 5e shows the SEM micrograph of the

composite after potentiodynamic polarization test in Red Sea water with more stained regions all over the surface of the composite. In general the Red Sea water contains other salts of Ca, S, K and so on. The EDAX profile (5f) clearly reveals the peaks of Ca and S apart from Na and Cl. The inference is that the composite surface reacts more with the electrolyte of Red Sea Water whereas the same show lower tendency of reaction in sodium chloride solution. Figure 5g and 5h show the SEM micrographs of composite specimens after 20 days exposure to 3.5 M sodium chloride solution and Red Sea water respectively. In both cases the interfacial regions between the reinforcement and the matrix are corroding since these regions are higher energy regions with semi-coherent nature [6,15,21].

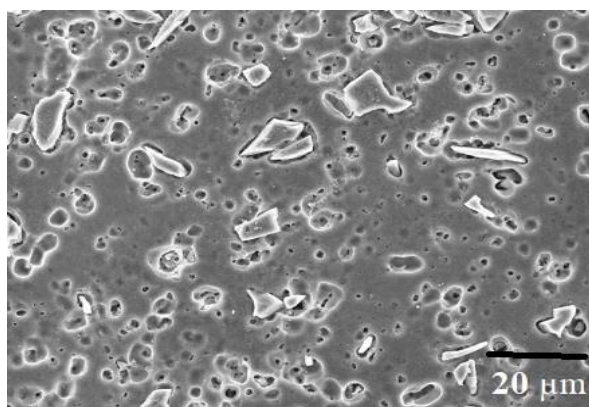


Figure 6. Peak Aged Composite

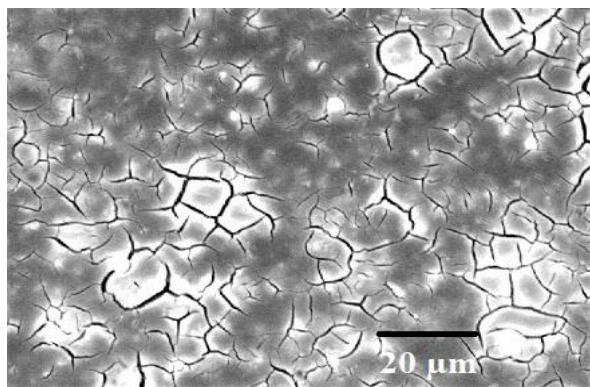


Figure 7. Peak Aged Composite Coated With CeO₂

The electrochemical performance of the CeO₂ covered composite was studied by analyzing polarization curves generated in 3.5 M NaCl aqueous solution and Red Sea Water. PA composite in NaCl solution and Red Sea Water as well as in the CeO₂ coated peak aged composite are presented in Figure 8 showing the corresponding cathodic and anodic curves. When the specimens were removed from the chemical bath, wet cerium hydroxide films were present over the specimens. The wet cerium hydroxide layers dry to form a crack-bound cerium oxide layer on the specimens when exposed to the ambient condition. The polarization curves of the CeO₂ covered composites are observed to shift in a positive direction. The samples that have been coated by ceria have a decreased current density (i_{corr}).

This reveals that the CeO_2 coating greatly improves the corrosion resistance of the peak-aged composite. The CeO_2 coated composite samples exhibit the similar behavior in terms of polarization resistance (R_p). When the corrosion features of the composite covered with ceria are compared to those of aged composite specimens, this is readily apparent.

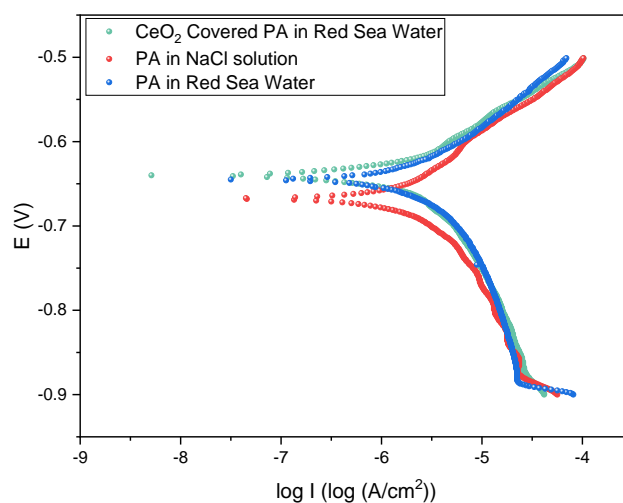


Figure 8. Potentiodynamic polarization plots of the aged composite and CeO_2 covered composite.

4. CONCLUSIONS

By a systematic stir casting technique the 7075 Al/ B_4C particulate reinforced composite material is prepared and the SEM metallography reveals that the reinforcement distribution in the matrix is nearly uniform. The precipitation hardening heat treatment and the hardness tests of the composite show that the highest hardness value can be attained at a temperature of $120\text{ }^\circ\text{C}$ and time period of 60 hours. The Potentiodynamic polarization analysis of the composite coupons in 3.5 M sodium chloride solution and Red Sea Water demonstrate that the PA composite specimen's exhibit lower corrosion resistance in comparison with the other intermediate temperature aged groups. Topographical analysis of the precipitation hardened composite specimens reveals that the corrosion reactions take place all over the matrix of the composite. Also the interfacial regions of the matrix corrode selectively. The galvanic corrosion of the matrix leads to pits formations on the matrix. The ceria conversion coating technique results in a crack bound but evenly existing CeO_2 layer on the composite. The corrosion rate of the peak aged composite in Red Sea Water drops by nearly 60 % when cerium oxide coating is applied.

References

1. Ruixiao Zheng, Xiaoning Hao, Yanbo Yuan, Zhiwei Wang, Kei Ameyama and Chaoli Ma, *Journal of Alloys and Compounds*, 576 (2013) 291-298.
2. V.V. Ganesh and N. Chawla, *Materials Science and Engineering: A*, 391 (2005) 342-353.
3. C. Carreño-Gallardo, I. Estrada-Guel, C. López-Meléndez, E. Ledezma-Sillas, R. Castañeda-Balderas, R. Pérez-Bustamante and J.M. Herrera-Ramírez, *Metals*, 8 (2018) 8647.

4. M.K. Surappa, *Sadhana*, 28 (2003) 319–334.
5. H.G. Rana, V.J. Badheka and A. Kumar, *Procedia Technology*, 23 (2016) 519-528.
6. S. Rajasekaran, N.K. Udayashankar and J. Nayak, *Surf. Engin. Appl. Electrochem.*, 47 (2011) 176.
7. Jaswinder Singh and Amit Chauhan, *Journal of Materials Research and Technology*, 5 (2016) 159-169.
8. Mario Bragaglia, Roberto Montanari and Giampiero Montesperelli, *Corrosion Engineering, Science and Technology*, 54:7 (2019) 601-613.
9. S. Rajasekaran, N.K. Udayashankar, and Jagannath Nayak, *ISRN Materials Science*, 2012 (2012).
10. B. Dikici, M. Gavgali and C. Tekmen, *Journal of Composite Materials*, 40 (2006) 1259-1269.
11. M. Sravanthi and K.G. Manjunatha, *Materials Today: Proceedings*, 5 (2018) 22581-22594.
12. Aisha H. Al-Moubaraki, Awatif Al-Judaibi and Maryam Asiri, *International Journal of Electrochemical Science*, 10 (2014) 4252-4278.
13. R. Flores-Campos, D.C. Mendoza-Ruiz, P. Amézaga-Madrid, I. Estrada-Guel, M. MikiYoshida, and J.M. Herrera-Ramírez, *J Alloys Compd.*, 495(2) (2010) 394–398.
14. Robert Baboian, 2nd Edition, ASTM Internationals, 2005.
15. Yahya Ali Fageehi, Rajasekaran Saminathan, Gunasekaran Venugopal, James Valder, Hemanth Kumar and K.S. Ravishankar, *Materials Today: Proceedings*, 42 (2021) 343-349.
16. Y.C. Lin, Jin-Long Zhang, Guan Liu and Ying-Jie Liang, *Materials & design*. 83 (2015)
17. Kaka Ma, Haiming Wen, Tao Hu, Troy D. Topping, Dieter Isheim, David N. Seidman, Enrique J. Lavernia and Julie M. Schoenung, *Acta Materialia*, 62 (2014) 141-155.
18. Adeyemi Dayo Isadare, Bolaji Aremo, Mosobalaje Oyebamiji Adeoye, Oluyemi John Olawale, and Moshood Dehinde Shittu, *Materials Research*, 16 (2013) 190-194.
19. T. Meng-Shan, S. Pei-Ling, K. Po-We and C. Chih-Pu, *Materials Transactions*, 50(4) (2009) 771-775.
20. J.F. Li and Z.W. Peng, *Transactions of Nonferrous Metal Society of China*, 18(4) (2008) 755-62.
21. Jin-feng Li et.al, *Transactions of Nonferrous Metals Society of China*, 18 (2008) 755-762.